NASA Technical Memorandum 84923

Mach Number and Flow-Field Calibration at the Advanced Design Propeller Location on the JetStar Airplane

Lannie D. Webb

December 1985

National Aeronautics and
Space Administration

NASA Technical Memorandum 84923

Mach Number and Flow-Field Calibration at the Advanced Design Propeller Location on the JetStar Airplane

Lannie D. Webb
Ames Research Center, Dryden Flight Research Facility, Edwards, California

1985

National Aeronautics and
Space Administration
Ames Research Center
Dryden Flight Research Facility
Edwards, California 93523

SUMMARY

Advanced design propellers on a JetStar aircraft were tested at NASA Ames Research Center's Dryden Flight Research Facility. A calibration of the flow field at the test location to obtain local Mach number and flow direction was performed. A pitot-static probe and flow direction vane installation was installed and tested at Mach 0.3 to 0.8 and altitudes from 3000 m (10,000 ft) to 9100 m (30,000 ft). Local Mach number and flow direction relationships were obtained and related to their noseboom counterparts. Effects of varying angles of sideslip to ±3° were investigated.

INTRODUCTION

Advanced design propellers were tested in flight on the JetStar Airplane at Nasa Ames-Dryden to obtain acoustic data (refs. 1, 2, and 3). The experimental propellers and drive motor were attached to the top of a pylon on the fuselage for testing. Comparison of acoustic data with wind tunnel data requires that the local Mach number and angle of attack at the propeller be accurately known. Therefore, a flow-field survey was conducted in the vicinity of the propeller location. This was accomplished by replacing the propeller installation on the pylon with a combined pitot-static probe and angle-of-attack vane. The pitot-static probe was located so that the static orifices were near the same coordinates as the center of the propeller blades and in the plane of rotation. Since the advanced propeller acoustic flights could not be flown with the pylon pitot-static system installed, it was necessary to reference the flow-field measurements made near the pylon to conditions measured by the noseboom-mounted pitot-static probe.

Two flow-calibration flights were made over the subsonic Mach number range and altitude test conditions used for the propeller tests. Corrected noseboom Mach number and angle of attack were used for comparison to measurements made on the pylon. The effects of sideslip on the local pylon flow field were ascertained. In addition, data were obtained to validate the position-error calibration of the noseboom pitot-static probe. This report summarizes the results of the JetStar pylon flow-field study and the verification of the noseboom airspeed calibration.

NOMENCLATURE

H	geometric altitude, m (ft)
M_{NB}	indicated noseboom Mach number
M_P	corrected pylon Mach number (corrected for isolated probe effects)
M'_P	indicated pylon Mach number
M_∞	free-stream Mach number
PCM	pulse code modulation

RSS	root sum square
α_{NB}	noseboom-measured angle of attack, deg
α_P	pylon-measured angle of attack, deg
β_{NB}	noseboom-measured angle of sideslip, deg
ΔM_{NB}	free-stream Mach number minus indicated noseboom Mach number, $M_\infty - M_{NB}$
ΔM_P	free-stream Mach number minus corrected pylon Mach number, $M_\infty - M_P$
$\Delta M'_P$	free-stream Mach number minus indicated pylon Mach number, $M_\infty - M'_P$
$\Delta\alpha$	noseboom-measured angle of attack minus pylon-measured angle of attack, $\alpha_{NB} - \alpha_P$, deg

DESCRIPTION OF APPARATUS

Test Aircraft

The aircraft used for testing advanced design propellers was the NASA Ames-Dryden JetStar airplane (fig. 1). The JetStar is a four-engined, medium-range jet transport that accommodates up to 10 passengers. The aircraft is powered by four JT12A-6 turbojet engines. Maximum takeoff weight of the airplane is 186,820 N (42,000 lb). For the advanced design propeller tests, a pylon was mounted on the upper fuselage surface of the JetStar (fig. 1(a)). The pylon was offset from the vertical centerline by 8° (fig. 1(b)). The advanced design propellers and an air turbine drive motor were mounted on the pylon for the acoustic tests; the propeller plane was 6.85 m (22.46 ft) from the nose.

Noseboom Air-Data Probe

The air-data probe consists of a pitot-static probe combined with a flow direction vane system. This probe, used on the noseboom of the JetStar airplane, was designed for use on research aircraft (ref. 4). Wind tunnel tests confirmed the small sensitivity of the static pressure orifices to changes in angles of attack up to 15°. The two free-floating vanes are used for accurate angle-of-attack (α_{NB}) and sideslip (β_{NB}) measurements.

Pylon Air-Data Probe

Combined pitot-static probe and flow vanes of the same type used on the noseboom were mounted on the pylon (fig. 2) in place of the propeller air turbine drive motor. The centerline of the pitot-static probe was aligned parallel to the centerline of the removed propeller air turbine drive motor, which was inclined 3° downward from the fuselage reference line (fig. 3). The static pressure orifices lie in the same vertical plane as the propeller plane of rotation. They are displaced approximately 10.2 cm (4 in) below the centerline and 6.85 m (22.5 ft) aft of the nose of the airplane (fig. 3). Unlike the noseboom installation where both angle of attack and

sideslip were measured, only angle of attack was measured on the pylon. Detailed information on construction and wind tunnel testing of the air-data probes used can be found in reference 4.

INSTRUMENTATION AND ACCURACY

Pressure Transducers

Pressure measurements on the noseboom and pylon were made with high-accuracy digital-output pressure transducers described in table 1. Differential transducers were used to measure the pressure between the total and static orifices on each probe. In addition, the static pressures were measured by absolute transducers. Airspeed and altitude were obtained from the differential and absolute measurements, respectively. The resolution of the 20-bit and 13-bit absolute transducers were 0.03 m/count (0.1 ft/count) and 3.4 m/count (11 ft/count), respectively; for the 20-bit differential (airspeed) transducers, a resolution of 0.096 N/m^2/count (0.002 lb/ft^2/count) was achieved. Indications of the uncertainty in these measurements were obtained from laboratory calibrations, hanger calibrations made just prior to the flow survey flights, and preflight and postflight ambient pressure checks. The estimated uncertainties are also shown in table 1, first for the airspeed and altitude measurements, and then for Mach number calculated from these values. The noseboom and pylon Mach number uncertainties, calculated using maximum instrumentation errors, are ± 0.001 and ± 0.004, respectively.

Flow Vanes

The resolution of the free-floating angle-of-attack and sideslip vanes (pylon sideslip vane disconnected) on the noseboom and pylon ranges from 0.02 to 0.03 deg/count. The estimated instrumentation uncertainty in the vane measurements was $\pm 0.25°$. The instrumentation uncertainty consists of nonflow-field measurement errors (such as calibration of the flow vane potentiometers, calibration of the boom bending, and misalignment of the vanes on the aircraft).

Data Recording

The analog output from the flow vanes was encoded by a pulse code modulation (PCM) system. An analog-to-digital converter in this system provided 10-bit resolution of the data. The data from the digital-output pressure transducers bypassed this converter, hence the full 20-bit (or 13-bit) pressure data were encoded directly into the PCM system. The data were sampled five times a second during the flow-field survey portion of the program, and were recorded on board the aircraft and telemetered to the ground.

TEST PROCEDURES

Two flights were flown with the propeller and drive motor removed and the pitot-static probe and angle-of-attack vane installed. During the flights, steady conditions were maintained for 1 min or more, which eliminated any uncertainties resulting

from pressure lag. The pilot flew test points at altitudes (H) of 3000 m (10,000 ft), 6100 m (20,000 ft), 7600 m (25,000 ft), and 9100 m (30,000 ft), and over a freestream Mach number (M_∞) range from 0.3 to 0.8. At a specific altitude the airplane was accelerated and decelerated to preselected Mach number and angle-of-sideslip combinations and then stabilized for data acquisition. During these stablized times, the airplane was at trim conditions of α_{NB}. The majority of test points were at 0° β_{NB}. Several angle-of-sideslip excursions were performed at ±1.5°, ±2°, and ±3°. The sideslip points were flown to define the pressure and flow angle changes at the pylon propeller location for $\beta_{NB} \neq 0°$ conditions.

During both flights, precision radar and rawinsonde balloon data were obtained for use in calculating Mach number position error for the pitot-static probe on the noseboom. This calibration verified a previous calibration of the noseboom air-data system. Using a calibrated U.S. Air Force T-38 PACER airplane, a series of PACER points were also taken. The PACER aircraft has dual sets of altimeters and airspeed sensors, to provide data to obtain position error calibration. The PACER points were taken at H ≈ 6100 m (20,000 ft) and 9100 m (30,000 ft), and spanned a Mach number range from 0.5 to 0.8.

Concurrent with the acquisition of data to verify the noseboom Mach number position error, data from the pylon pitot-static probe were also recorded. The ratio of differential to static pressure from the pylon probe was used to calculate the pylon Mach number (M'p). Isolated probe corrections from reference 4 were applied to M'p, and the corrected Mach number M_p was subtracted from M_∞ to get ΔM_p.

Corrections to the angle-of-attack vane for an isolated vane and pitot-static probe combination are zero for $\alpha_{NB} = \beta_{NB} = 0°$ and up to $M_\infty \approx 0.85$ (ref. 4). For $\alpha_{NB} \approx 5°$ and $\beta_{NB} \approx \pm 3°$, a correction to α_{NB} of -0.25° is indicated (ref. 4) for $M_\infty = 0.60$ and 0.80. The same tests indicated corrections to β_{NB} of approximately 0.1° to 0.2° at $M_\infty = 0.60$ and 0.80 for $\alpha_{NB} = 0°$. In general, for the flight conditions of primary interest (that is, $M_\infty \approx 0.80$ and $\beta_{NB} \approx 0°$), the isolated-vane corrections are very small. Since the magnitude of the isolated-vane corrections are less than the vane measurement uncertainties, and the upwash corrections at $M_\infty \approx 0.80$ were neglected, vane corrections were not warranted.

ERROR ANALYSIS

Free-Stream and Pylon Mach Numbers

In addition to the instrumentation errors, several other sources of uncertainty combine to make up the total uncertainty in the calculations of the free-stream Mach number of the JetStar airplane. These uncertainties are introduced during establishment of the noseboom position-error curve. The main elements making up the uncertainty in the position-error curve are: (1) the stability of the PACER and test aircraft during the calibration runs, (2) the accuracy of the radar, and (3) the accuracy of the weather data.

Figure 4 shows the difference between free-stream and indicated noseboom Mach numbers (ΔM_{NB}) as a function of indicated noseboom Mach number (M_{NB}). A fairing was made through the PACER aircraft and radar data. The scatter of the data around this fairing is ±0.002 to ±0.003, which is thought to be representative of the total uncertainty of the curve. The noseboom uncertainties and their root sum square (RSS) values of ±0.003 are summarized in table 2. For the pylon Mach number, the overall uncertainty is due to the combined instrumentation uncertainties and the noseboom uncertainties. This result is shown in table 3, and amounts to an overall uncertainty of ±0.005 in local Mach number at the pylon.

Flow Angularity

The uncertainty in determining the angularity of the flow field just ahead of the pylon on the aircraft can be attributed to two primary sources of error: (1) the uncertainty of the noseboom-measured angle of attack, (α_{NB}) and (2) the uncertainty in relationship of α_{NB} with $\Delta\alpha$ (the difference between noseboom- and pylon-measured angle of attack). The instrumentation uncertainty in the noseboom-measured angle of attack is ±0.25°. By combining this with the slope and scatter in the pylon-versus-noseboom angle-of-attack relationship, an overall uncertainty of ±0.32° was determined for the pylon-measured angle of attack. This analysis was made using data for Mach numbers of 0.6 to 0.8. Because the region of prime concern for propeller testing is near the upper end of this Mach number range, noseboom vane upwash, which may be significant at lower Mach numbers, was neglected.

RESULTS

Noseboom Position Error

Noseboom position-error calibration data were obtained with the data gathered for describing the pylon flow field. Radar tracking data, used in conjunction with weather balloon data, were obtained for both calibration flights. The method referred to in reference 5, appendix B, was used to determine the relationship between radar pressure altitude and pressure altitude from available rawinsonde data. On one flight it was necessary to adjust the pressure altitude by the Edwards Air Force Base rawinsonde data, by approximately 20 m (60 ft). However, no adjustment was necessary for the rawinsonde data closest to flight time on the other flight.

In addition to the radar data, 20 stabilized PACER aircraft points were obtained. Figure 4 compares the original position-error calibration (solid line) with the radar and PACER data from the present series of tests. Radar data were selected for use only when the elevation angle was 8° or larger to minimize refraction errors. A fairing (dashed line) was made through all the new points (fig. 4). The fairing lies below the original position calibration by 0.003 to 0.004. This does not represent a substantial change in the noseboom position-error curve. The original position-error calibration curve is used to calculate M_∞ for comparison with the advanced design propeller data. In this report, the revised curve (fig. 4) was used for calculating M_∞ in figures 5, 6, 7, 10, and 11.

Pylon Local Flow Conditions

Variation of $\Delta M'_p$ with M_∞ ($\beta \approx 0°$). – The variation of $\Delta M'_p$ (free-stream minus indicated pylon Mach number) with M_∞ for several test altitudes is shown in figure 5. For free-stream Mach numbers less than approximately 0.65, the pylon Mach numbers are higher than free-stream Mach numbers, while the reverse is true for conditions above $M_\infty > 0.65$. Also shown in the figure are fairings of lines of approximate angles of attack associated with the flight points. In general, the low angle-of-attack points are above the $\Delta M'_p = 0$ line, while the high angles of attack lie below.

In figure 5, most of the data fall into three groups, which correspond to the three primary altitudes of the calibration tests. The relationships (fig. 5) are primarily the result of two factors: (1) the pitot-static probe location atop the pylon on the JetStar airplane, and (2) the various combinations of M_∞ and α_{NB} that occur at the three test altitudes. The combinations of M_∞ and α_{NB} cause the local pressures around the pylon to vary above or below the free-stream pressure, causing $\Delta M'_p$ to become either positive or negative (fig. 5). For free-stream Mach numbers below approximately 0.65, the local M'_p is higher than M_∞ because of flow expansion over the top of the fuselage. As M_∞ approaches 0.8, the magnitude of $\Delta M'_p$ increases rapidly. This is probably the result of the formation and strengthening of local shock waves on the fuselage. Even with the rapid increase in $\Delta M'_p$ near $M_\infty = 0.8$, the final corrected pylon Mach numbers were found to be very close to those for free-stream Mach number conditions.

Variation of $\Delta M'_p$ with α_{NB} ($\beta \approx 0°$). – Since the type of pitot-static probe used on the noseboom and pylon was designed to relatively insensitive to angle-of-attack variations, the relationships found in figure 5 require further explanation. For this analysis, only values of $\Delta M'_p$ lying near $M_\infty \approx 0.72$ and two test altitudes were selected. Figure 6 presents $\Delta M'_p$ as a function of α_{NB} at $M_\infty \approx 0.72$ and $\beta \approx 0°$. The figure shows a linear relationship between $\Delta M'_p$ and α_{NB} for the flight conditions selected. This is shown pictorially in the top half of figure 6.

Variation of $\Delta M'_p$ with β_{NB}. – The variation of $\Delta M'_p$ with angle of sideslip β_{NB} at $M_\infty \approx 0.72$ is illustrated in figure 7. Data presented are for the range of $\beta_{NB} \approx \pm 3°$ and for two angle-of-attack ranges. The two curves in figure 7 exhibit apparent symmetry about $\beta_{NB} \approx 1°$ instead of 0°. This is probably because the pylon was offset from the vertical centerline by 8° (fig. 1(b)). For example, a change of 0.005 in $\Delta M'_p$ occurs between $\beta_{NB} \approx 1°$ and $\beta_{NB} \approx -3°$ for angles of attack between 2° and 3°. With increased angle of attack, the values of $\Delta M'_p$ at $\beta_{NB} \approx 0°$ become more negative (not shown), and the shapes of the curves probably remain similar to the two in figure 7.

Pylon Flow Angularity

Flow angularity ($\beta_{NB} \approx 0°$). – The flow angularity in the region of the pylon is shown in figure 8. Figure 8 illustrates the difference of $\Delta\alpha$ between α_{NB} and local pylon flow angle (α_p) as a function of α_{NB} for $\beta_{NB} \approx 0°$. The curve is referenced to

the centerline of the propeller drive motor. When plotted, the data obtained at all three primary test altitudes formed a single curve, which indicates that there are no significant effects of Mach number or altitude on the flow angle vanes for the conditions tested. The α_p was always positive and less than α_{NB}.

Flow angularity ($\beta_{NB} \neq 0°$). – Figure 8 related $\alpha_{NB} \neq 0°$ as a function of $\Delta\alpha_{NB}$, where $\beta_{NB} \approx 0°$. While in figure 9, the same parameters (α_{NB} and $\Delta\alpha_{NB}$) are plotted for several $\beta_{NB} \neq 0°$. Data were obtained at $\beta_{NB} \approx \pm 1.5°$, $\pm 2.0°$, and $\pm 3.0°$, respectively. Figure 9 illustrates that changes in β_{NB} can have significant effects on Δa and, therefore, on the local flow angle α_p. For example, when β_{NB} is $-2°$, the local flow angle α_p is larger by about $0.5°$ than it is when $\beta_{NB} \approx 0°$ (fig. 8). When β_{NB} is $2°$, the local flow angle α_p is less than the local flow angle for $\beta_{NB} \approx 0°$ by approximately $0.75°$. Larger effects can be deduced from the limited data for $\beta_{NB} \approx \pm 3°$ (shown in fig. 9).

Isolated Probe Corrections

The local Mach numbers measured by the pylon pitot-static probe are affected by the flow field of the aircraft and the pylon, and by the induced flow field of the probe. Since the first two effects are present when the various advanced design propeller blades are tested, these corrections are not needed. The remaining effect (that is, the flow field of the isolated pitot-static probe) was small (less than 0.008 Mach), but was corrected using wind tunnel data from reference 3. Corrections from the wind tunnel tests (table 4) were added to the indicated pylon Mach number (M'_p) to obtain the corrected pylon Mach number (M_p).

Summary Calibration Curves

For quick user reference, ΔM_p, M_p, and α_p were replotted as a function of M_∞ and α_{NB} for the flight conditions of most interest.

Variation of ΔM_p with M_∞ ($\beta \approx 0°$). – Figure 10 shows M_p subtracted from M_∞ and the faired difference ΔM_p plotted as a function of M_∞. After the corrections were made for isolated probe effects, the pylon Mach numbers were found to be larger than free-stream Mach numbers up to $M_\infty = 0.76$. These corrections also resulted in the values of ΔM_p being close to those for free-stream conditions between $M_\infty \approx 0.70$ and 0.80. For this Mach number range, the values of ΔM_p vary in magnitude approximately ± 0.005 around $M_\infty = 0.76$, which is very close to the measurement accuracy. The Mach numbers M_p are representative of the disturbed flow that was present during testing of the advanced design propellers.

Mach number ($\beta_{NB} \approx 0°$). – In figure 11 the data from figure 10 are shown replotted with M_p as a function of M_∞. The data cover the range from $M_\infty = 0.76$ to $M_\infty = 0.82$ at $H \approx 9100$ m (30,000 ft) and $\beta_{NB} \approx 0°$. Using the condition $M_\infty = 0.80$ as an example, the corrected Mach number at the pylon is $M_p = 0.794$. The calibration

indicates that for $M_\infty > 0.76$, the pylon Mach number will be less than free-stream Mach number. Corrected pylon Mach numbers for the range $M_\infty = 0.50$ to 0.82 are listed in table 5.

Flow angularity ($\beta \approx 0°$). – Figure 12 relates α_{NB} with α_p directly from the data plotted in figure 8. For all the flight conditions, the local flow angles at the pylon are less than the free-stream angle of attack, and are always positive. For example, for the JetStar flight conditions of primary interest during the testing of the advanced design propellers (that is, $M_\infty \approx 0.80$, and $2.7° \approx \alpha_{NB} \approx 3°$), α_p ranges between 0.9° and 1.1°.

CONCLUDING REMARKS

The flow field at the location of advanced design propellers on the JetStar airplane was studied. The Mach number uncertainty was ±0.003 at the noseboom and ±0.005 at the propeller location. The noseboom position-error calibration was determined and found to be very close to a previous calibration. At free-stream Mach numbers below 0.760, pylon Mach number (corrected for isolated probe effects) was higher than free stream. At Mach numbers above 0.760, pylon Mach number was slightly less than free stream.

Local angle of attack at the pylon was less than free-stream angle of attack, and was always positive. For example, at the flight point of most interest (Mach 0.8 at an altitude of 9100 m (30,000 ft)), the local Mach number at the propeller location was 0.794, and the local angle of attack was between 0.9° and 1.1°.

The effect of changing angles of attack and sideslip on pylon Mach numbers and flow angles was small. In most instances, the changes were close to the uncertainties in the primary measurements.

Ames Research Center
Dryden Flight Research Facility
National Aeronautics and Space Administration
Edwards, California, August 18, 1983

REFERENCES

1. Dittmar, James H.; and Lasagna, Paul L.: A Preliminary Comparison Between the SR-3 Propeller Noise in Flight and in a Wind Tunnel. NASA TM-82805, 1982.

2. Mackall, K. G.; Lasagna, P. L.; Dittmar, J. H.; and Walsh, K.: In-Flight Acoustic Results From An Advanced-Design Propeller at Mach Numbers to 0.8. AIAA Paper 82-1120, 1982.

3. Walsh, Kevin R.: Flow Field Survey Near the Rotational Plane of an Advanced Design Propeller on a JetStar Airplane. NASA TM-86037, 1985.

4. Richardson, Norman R.; and Pearson, Albin O.: Wind Tunnel Calibrations of a Combined Pitot-Static Tube, Vane-Type Flow Direction Transmitter, and Stagnation-Temperature Element at Mach Numbers From 0.60 to 2.87. NASA TN D-122, 1959.

5. Larson, Terry J.; and Ehernberger, L. J.: Techniques Used for Determination of Static Source Position Error of a High Altitude Supersonic Airplane. NASA TM X-3152, 1975.

TABLE 1. — CHARACTERISTICS AND ACCURACY OF THE PRESSURE TRANSDUCERS, FOR JETSTAR FLOW-FIELD SURVEY

Pressure Transducers				Estimated maximum uncertainty at 9100 m (30,000 ft)		
Location	Parameter measured	Type and Resolution (bits)	Range kN/m^2 (lb/ft^2)	Pressure, N/m^2 (lb/ft^2)	Altitude, m (ft)	Mach number
Noseboom	Airspeed	Digital quartz (20)	±40.6 (±848)	±24 (±0.5)	No data	±0.001
Noseboom	Altitude	↓	17 to 271 (355 to 5660)	±48 (±1)	±8.5 to 10.7 (±28 to ±35)	±0.001
Pylon	Airspeed	↓	±40.6 (±848)	±24 to ±96 (±0.5 to ±2.0)	No data	±0.004
Pylon	Altitude	Digital quartz (13)	1.8 to 101 (37 to 2116)	±45.5 (±0.95)	±10 (±33)	±0.004

TABLE 2. — UNCERTAINTY IN NOSEBOOM MACH NUMBER, M_∞

Parameter	Symbol	Uncertainty
Noseboom instrumentation	A	±0.001
Test data (such as PACER, radar, and weather)	B	+0.003
RSS	$\sqrt{A^2 + B^2}$	±0.003

TABLE 3. – UNCERTAINTY IN PYLON MACH NUMBER, M_P

Parameter	Symbol	Uncertainty
Pylon instrumentation	A	±0.004
M_∞	B	±0.003
RSS	$\sqrt{A^2 + B^2}$	±0.005

TABLE 4. – CORRECTION TO PYLON MACH NUMBER FOR AN ISOLATED PROBE AT α_{NB} FROM 0° to 10° (FROM REF. 4)

M_P	β_{NB}		
	0°	1.5°	3°
0.2	---	---	---
0.3	---	---	---
0.4*	0.0013	---	---
0.5*	0.0022	---	---
0.6	0.0035	0.0026	0.0017
0.7	0.0056	---	---
0.8	0.0074	0.0068	0.0053

*Extrapolated

TABLE 5. – CORRECTED PYLON MACH NUMBERS FOR M_∞ = 0.500 to 0.820 AT H ≈ 9100 m (30,000 ft) and $\beta_{NB} \approx 0°$

M_∞	M_P	M_∞	M_P
0.500	0.512	0.730	0.733
0.550	0.562	0.740	0.742
0.600	0.611	0.760	0.760
0.650	0.660	0.780	0.777
0.700	0.706	0.800	0.794
0.710	0.715	0.820	0.811
0.720	0.724		

(a) Airplane with pylon-mounted propeller and noseboom air-data probe installation.

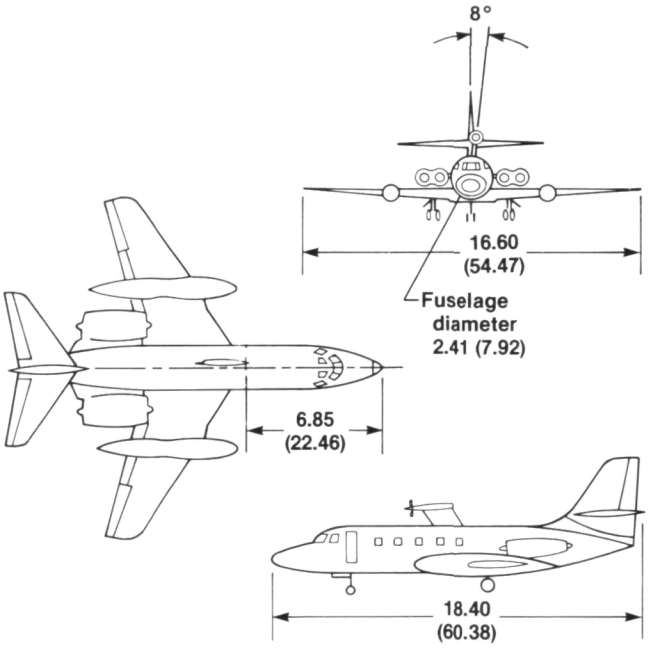

(b) Three-view diagram of propeller installation. Dimensions in meters (feet).

Figure 1. JetStar airplane.

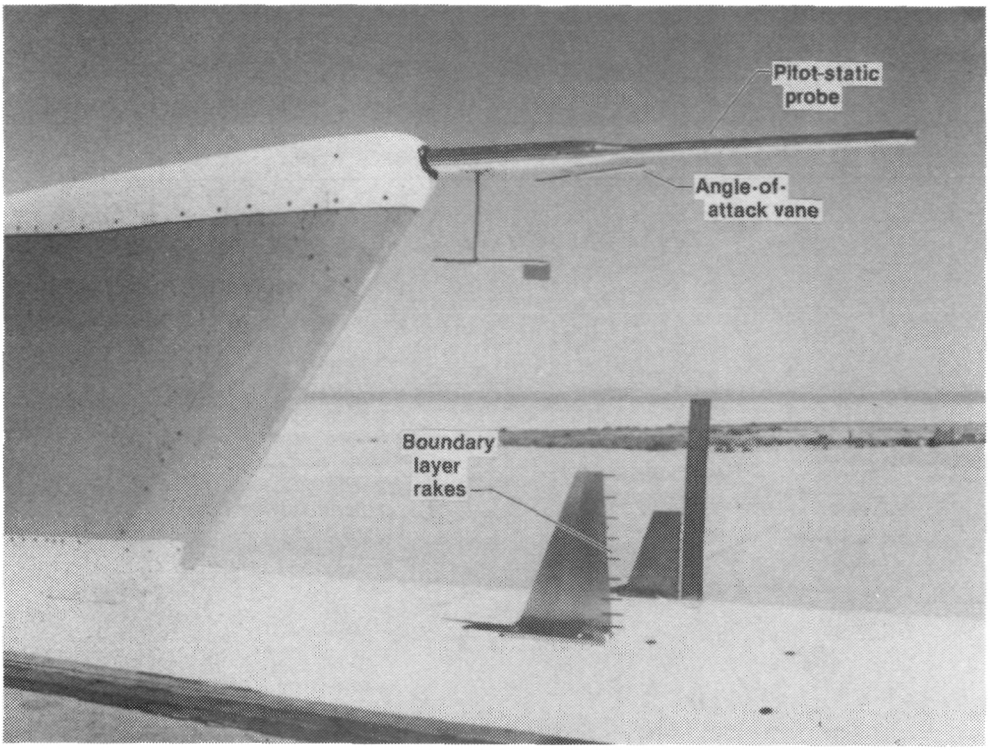

Figure 2. Pylon-mounted air-data probe.

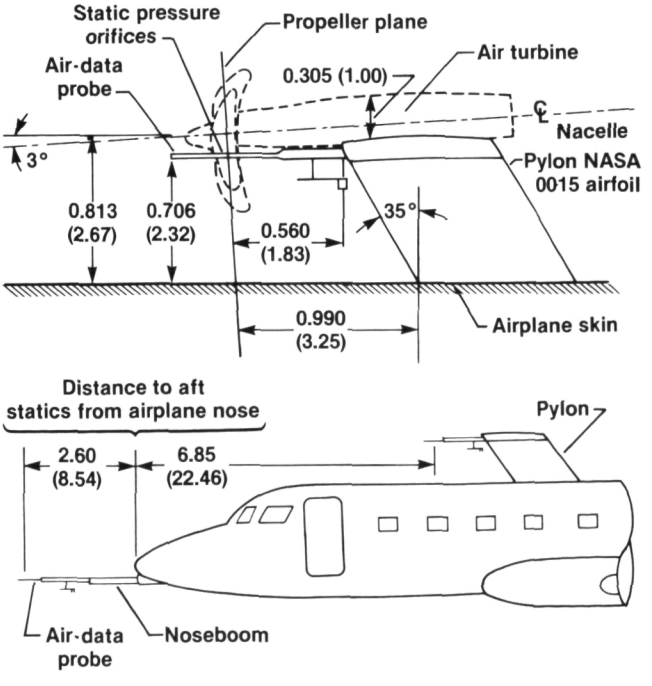

Figure 3. Schematic of pitot-static probe installations on the pylon and noseboom. Dimensions in meters (feet).

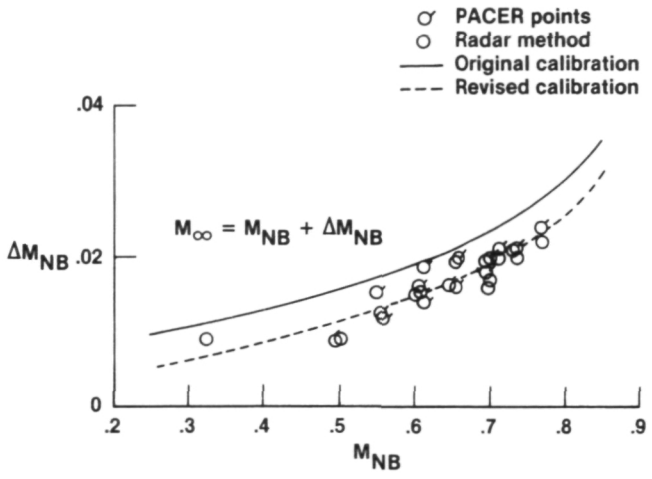

Figure 4. Noseboom airspeed calibration for an angle-of-attack range of 2.3° to 7.0° ($\beta_{NB} \approx 0°$).

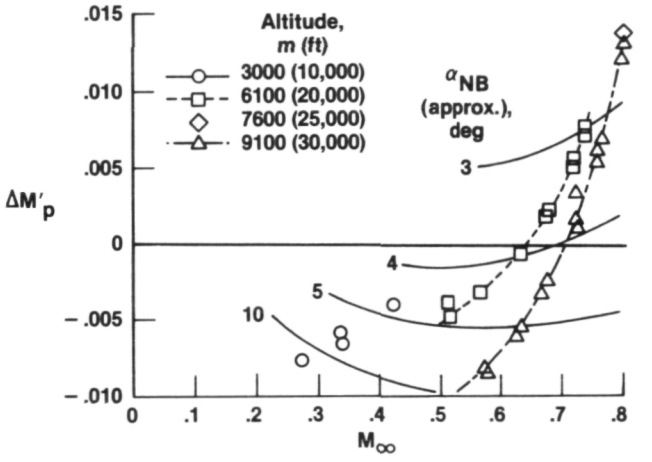

Figure 5. Variation of $\Delta M'_p$ with M_∞ for several test altitudes at $\beta_{NB} \approx 0°$.

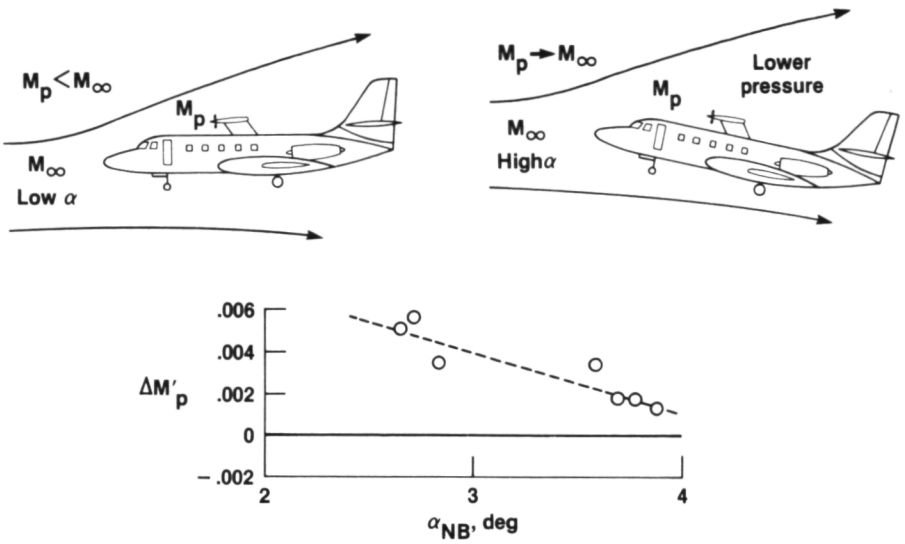

Figure 6. Variation of $\Delta M'_p$ with α_{NB} at $M_\infty \approx 0.72$ and $\beta_{NB} \approx 0°$.

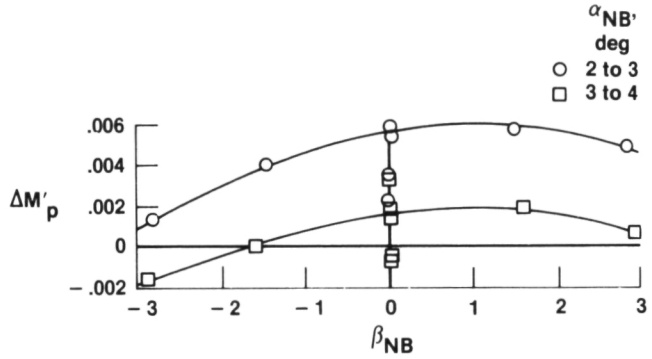

Figure 7. Variation of $\Delta M'_p$ as a function of β_{NB} for two α_{NB} ranges. $M_\infty \approx 0.72$.

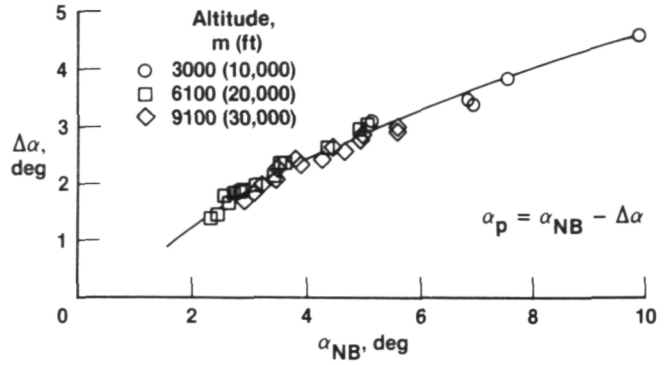

Figure 8. Variation of Δα referenced to the propeller centerline as a function of α_{NB} over the entire altitude and Mach number range tested ($\beta_{NB} \approx 0°$).

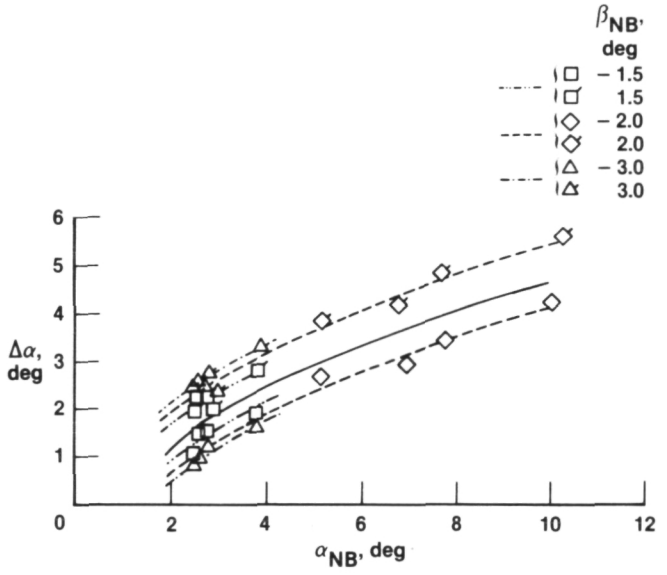

Figure 9. Variation of Δα with α_{NB} for $\beta_{NB} \approx \pm 1.5°$, $\pm 2°$, and $\pm 3°$.

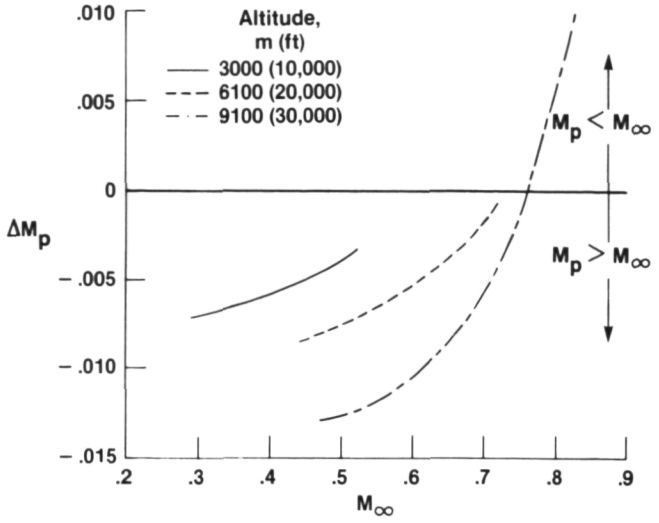

Figure 10. Variation of ΔM_p with M_∞ over several test altitudes at $\beta_{NB} \approx 0°$.

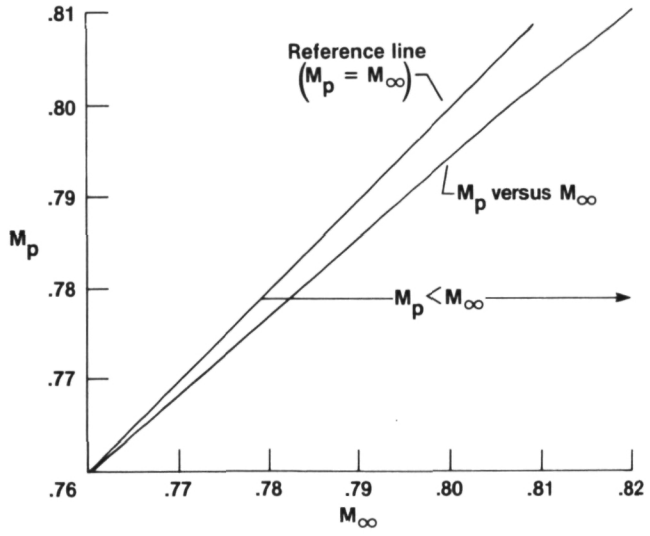

Figure 11. Variation of M_p with M_∞ for conditions near $M_\infty = 0.8$, H ≈ 9100 m (30,000 ft), and $\beta_{NB} \approx 0°$.

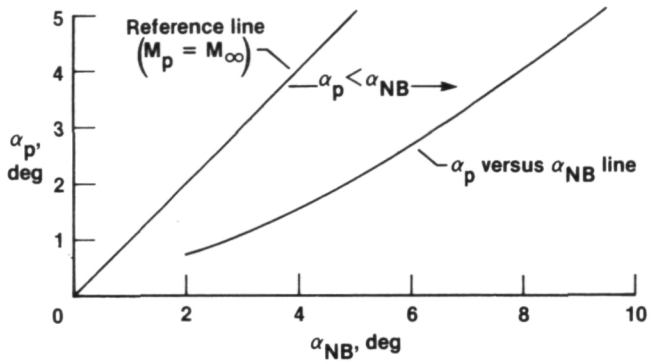

Figure 12. Variation of α_p as a function of α_{NB} over the entire altitude and Mach number ranges ($\beta_{NB} \approx 0°$).

1. Report No.	2. Government Accession No.	3. Recipient's Catalog No.
NASA TM-84923		

4. Title and Subtitle	5. Report Date
MACH NUMBER AND FLOW-FIELD CALIBRATION AT THE ADVANCED DESIGN PROPELLER LOCATION ON THE JETSTAR AIRPLANE	December 1985
	6. Performing Organization Code

7. Author(s)	8. Performing Organization Report No.
Lannie D. Webb	H-1222
	10. Work Unit No.
	RTOP 535-03-11

9. Performing Organization Name and Address	11. Contract or Grant No.
NASA Ames Research Center Dryden Flight Research Facility P.O. Box 273 Edwards, CA 93523	
	13. Type of Report and Period Covered
12. Sponsoring Agency Name and Address	Technical Memorandum
National Aeronautics and Space Administration Washington, D.C. 20546	14. Sponsoring Agency Code

15. Supplementary Notes

16. Abstract

Advanced design propellers on a JetStar aircraft were tested at NASA Ames Research Center's Dryden Flight Research Facility. A calibration of the flow field at the test location to obtain local Mach number and flow direction was performed. A pitot-static probe and flow direction vane installation was installed and tested at Mach 0.3 to 0.8 and altitudes from 3000 m (10,000 ft) to 9100 m (30,000 ft). Local Mach number and flow direction relationships were obtained and related to their noseboom counterparts. Effects of varying angles of sideslip to ±3° were investigated.

17. Key Words (Suggested by Author(s))	18. Distribution Statement
Local flow-field calibration JetStar airplane Advanced design propeller	Unclassified – Unlimited STAR category 02

19. Security Classif. (of this report)	20. Security Classif. (of this page)	21. No. of Pages	22. Price*
Unclassified	Unclassified	19	A02

For sale by the National Technical Information Service, Springfield, Virginia 22161.